NASA-CR-175105

487.

THERMIONIC NOISE MEASUREMENTS FOR ON-LINE DISPENSER CATHODE DIAGNOSTICS FOR LINEAR BEAM MICROWAVE TUBES

SRI Project No. 6923

Final Report

August 1985

By: Christopher E. Holland, Research Physicist
Ivor Brodie, Director
Physical Electronics Laboratory

Prepared for:

National Aeronautics and Space Administration
Lewis Research Center
21000 Brookpark Road
Cleveland, Ohio 44135

Attn: Mr. E.G. Wintucky
MS 54-5

Contract No. NAS3-23777

SRI International
333 Ravenswood Ave. • Menlo Park, CA 94025
(415) 326-6200 • TWX: 910-373-2046 • Telex: 334-486

1. Report No.	2. Government Accession No.	3. Recipient's Catalog No.

4. Title and Subtitle	5. Report Date
Thermionic Noise Measurements for On-Line Dispenser Cathode Diagnostics for Linear Beam Microwave Tubes	August 1985
	6. Performing Organization Code
7. Author(s)	8. Performing Organization Report No.
Christopher Holland and Ivor Brodie, PhD	Final Report SRI Project 6923
9. Performing Organization Name and Address	10. Work Unit No. (TRAIS)
SRI International 333 Ravenswood Avenue Menlo Park, California 94025	11. Contract or Grant No. NAS3-23777
12. Sponsoring Agency Name and Address	13. Type of Report and Period Covered
National Aeronautics & Space Administration Lewis Research Center 21000 Brookpark Road Cleveland, Ohio 44135	Final February 1984 - August 1985
	14. Sponsoring Agency Code

15. Supplementary Notes

16. Abstract

A test stand has been set up to measure the current fluctuation noise properties of B- and M-type dispenser cathodes in a typical TWT gun structure. Noise techniques were used to determine the work function distribution on the cathode surfaces. We find significant differences between the B and M types and significant changes in the work function distribution during activation and life. In turn, knowledge of the expected work function can be used to accurately determine the cathode-operating temperature in a TWT structure. Noise measurements also demonstrate more sensitivity to space charge effects than the Miram method. Full automation of the measurements and computations is now required to speed up data acquisition and reduction.

The complete set of equations for the space charge limited diode were programmed so that given four of the five measurable variables (J, J_0, T, d, and V) the fifth could be computed. Using this program, we estimated that an rms fluctuation in the diode spacing d in the frequency range of 145 Hz about 20 kHz of only about 10^{-5} Å would account for the observed noise in a space charge limited diode with 1 mm spacing.

17. Key Words	18. Distribution Statement

19. Security Classif. (of this report)	20. Security Classif. (of this page)	21. No. of Pages	22. Price
Unclassified	Unclassified		

ABSTRACT

A test stand has been set up to measure the current fluctuation noise properties of B- and M-type dispenser cathodes in a typical TWT gun structure. Noise techniques were used to determine the work function distribution on the cathode surfaces. We find significant differences between the B and M types and significant changes in the work function distribution during activation and life. In turn, knowledge of the expected work function can be used to accurately determine the cathode-operating temperature in a TWT structure. Noise measurements also demonstrate more sensitivity to space charge effects than the Miram method. Full automation of the measurements and computations is now required to speed up data acquisition and reduction.

The complete set of equations for the space charge limited diode were programmed so that given four of the five measurable variables (J, J_0, T, d, and V) the fifth could be computed. Using this program, we estimated that an rms fluctuation in the diode spacing d in the frequency range of 145 Hz about 20 kHz of only about 10^{-5} Å would account for the observed noise in a space charge limited diode with 1 mm spacing.

CONTENTS

ILLUSTRATIONS

TABLES

I BACKGROUND

Since the inception of microwave beam tubes there has been a clear need to conduct cathode diagnostics while the tube is still located in the communication system in which it is being operated.[1] * If it is known that the cathode is approaching the end of its useful life or approaching failure for any other reason, then the tube could be replaced at a convenient time rather than waiting for failure on line. This is especially true for traveling wave tubes (TWT's) used for satellite communications. Under such circumstances, the only measurement that can be made on the gun is the emission current as a function of voltage and heater power; even the cathode temperature cannot be observed directly.

To obtain a better understanding of the sensitivity of the cathode toward space charge effects, the complete set of equations for space charge limited operation were programmed in a computer. As a result, given four of the five measurable parameters (J, J_0, T, d, and V), the fifth could be computed. The theory used in this analyses is discussed in the appendix.

The work described in this report covers the initial phase of exploring the use of current fluctuation noise for TWT cathode diagnostics, particularly for barium dispenser cathodes designated B and M types.[2,3] In principle, the following parameters should be capable of being estimated from noise measurements.

- Work function distribution - from the variation of Γ^2 with the current.
- Cathode temperature - from the space charge reduction of the shot noise (Γ^2).
- Barium surface coverage (and hence the barium supply rate) - from the low frequency (flicker) noise spectrum.

The key tasks for this phase of the program were:

- Design, assemble and operate a test stand suitable for taking measurements on a range of TWT diode or triode gun structures.

*References listed at end of report.

- Detect and process the low-through high-frequency noise signals from B- and M-type cathodes operating in the above test stand.

- Provide preliminary analysis of the noise measurements to see how effectively the important cathode properties can be ascertained as a function of lifetime.

II EXPERIMENTAL METHOD

A. *Gun Structures*

The TWT guns used in this study were conventional TWT structures with B- and M-type cathodes. The gun structure was manufactured by MEC-Teledyne and designated type 68670. Figure 1 is a cross-sectional view of the gun. The B cathode consists of a tungsten matrix of 80% density impregnated with a 5:3:2 mole ratio of BaO, CaO, Al_2O_3. M-type cathodes were the same but with the emitting surface coated with osmium-ruthinium layers. The cathodes had an area of $4.56 \times 10^{-3} cm^2$.

A total of 6 different cathodes were tested during this program (4 B, 2 M). The first two (B-type) were used to establish operation parameters and determine a suitable measurement technique.

B. *Vacuum Apparatus*

The initial arrangement consisted of single gun element placed in an ion-pumped system (Figure 2). Feed-throughs were provided for all the grid elements. The system also included an electrostatic quadrupole deflector and phosphor screen to optimize the focusing characteristics. The quadrupole was used to deflect the beam and reduce the power density on the phosphor. The axis of the gun structure was situated so that the temperature could be monitored by an optical pyrometer through a vacuum viewing window.

In this configuration, the cathode temperature could be monitored while establishing optimum focusing parameters for the gun on the phosphor. However, although the quadrupole deflector was introduced to help reduce the power density on the phosphor, it still proved too high, and a spot was burned on the screen. It was then not possible to take any significant noise measurements under these conditions.

The gun was also operated under a pseudo diode configuration. Here all electrodes were tied to a common line. The lens elements thus acted as the anode. Under these

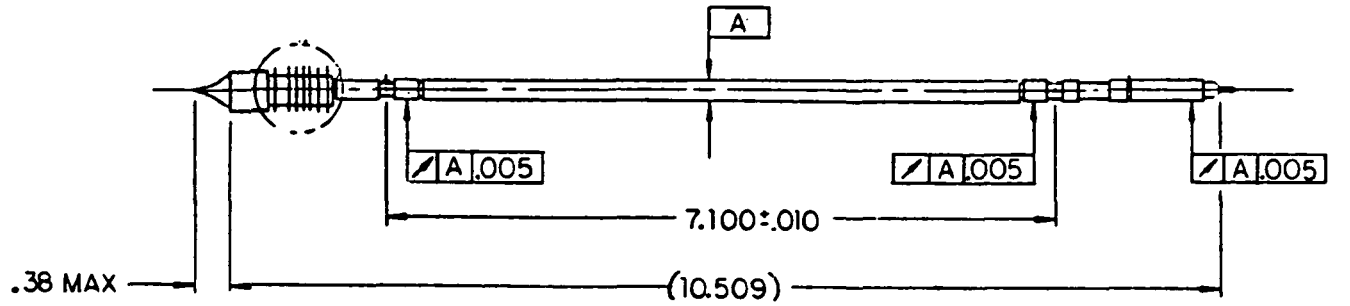

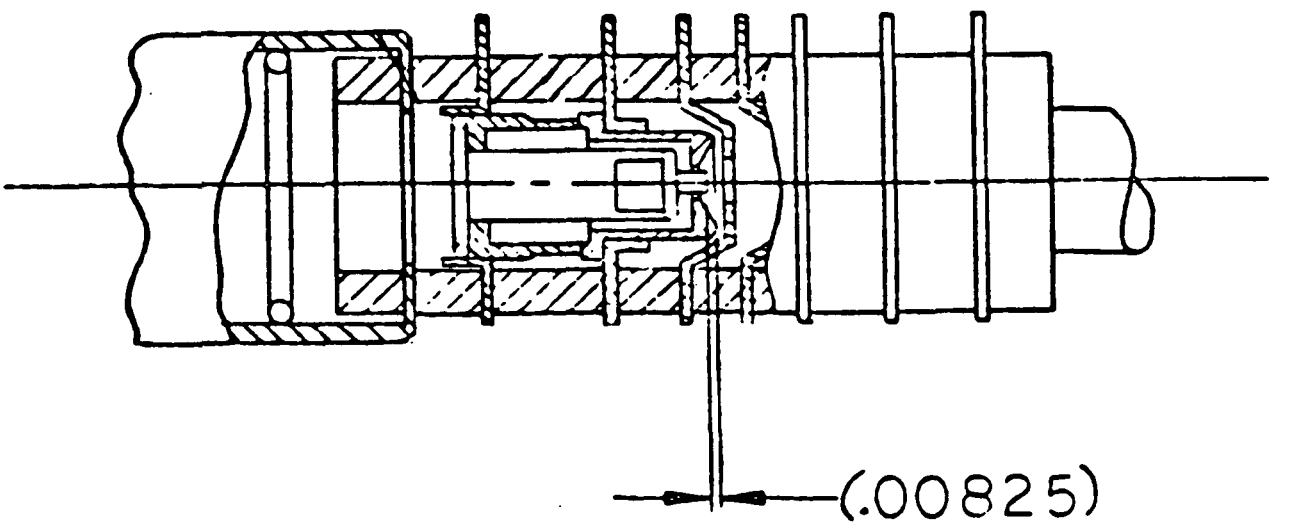

Figure 1 Cross-sectional view of MEC-Teledyne gun
(dimensions are in inches)

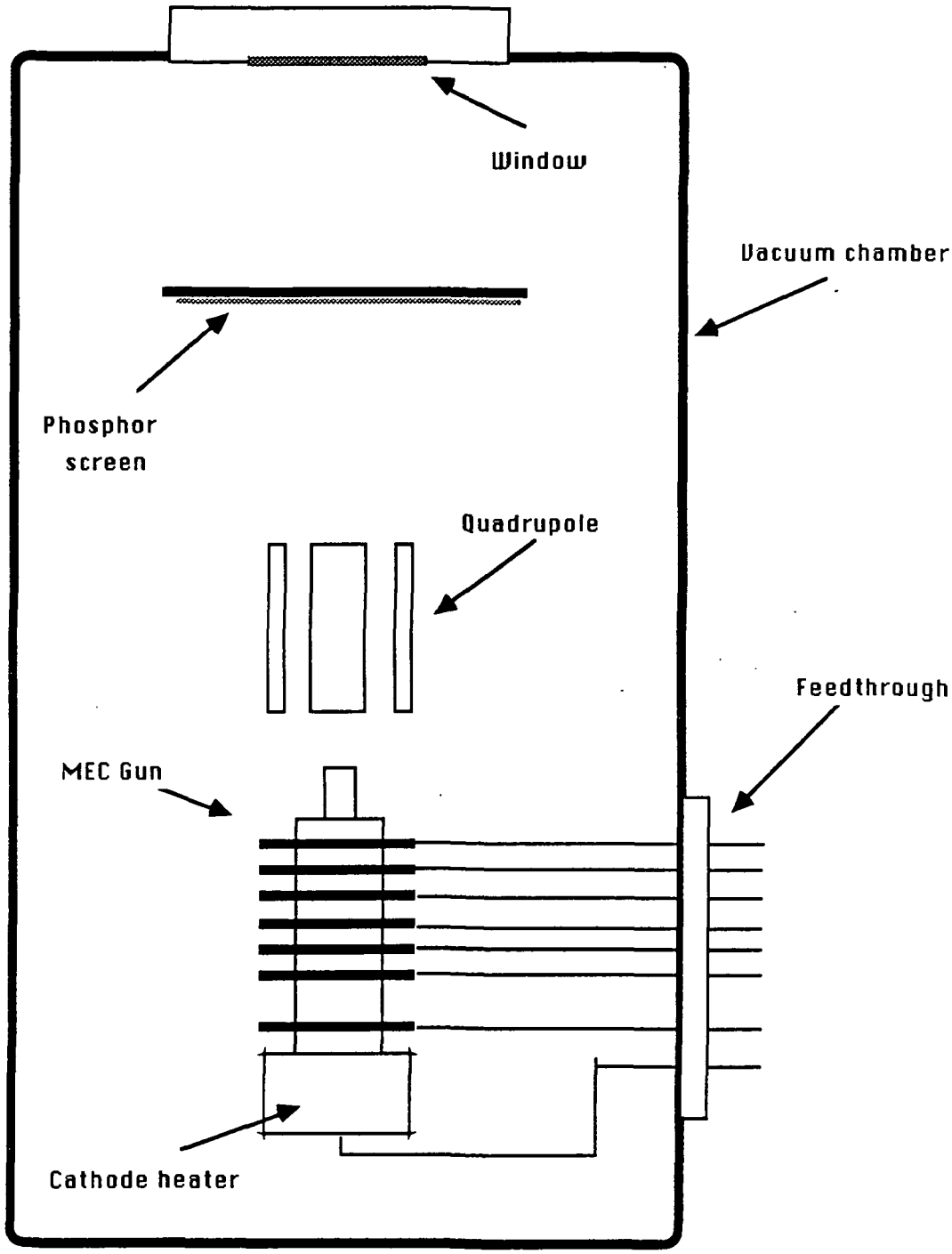

FIGURE 2 Initial vacuum system

conditions, it was possible to operate the cathode up to 1 A/cm^2 without overheating the lenses. This configuration was used to establish the current noise measuring instrumentation which is discussed in the following section II-C.

A second structure was assembled to operate the cathode and gun using the focusing parameters established in the first system. The gun was placed in a turbo-molecular pumped system. A high power anode was used in this scheme so that the system could operate under normal electrostatic focusing conditions. Figure 3 is a schematic of this apparatus. An electrode with a small aperture was placed in the anode so that the cathode temperatures could be viewed with an optical pyrometer through the window. The electrode was held at a retarding potential to prevent loss of electrons. The operating pressure in the system was $< 5 \times 10^{-9}$ as measured with an ionization gauge.

A third vacuum system was assembled to life test four (2 B-type, 2 M-type) gun structures in parallel. In this system, it was only possible to operate in the pseudo diode configuration. Again temperatures could be monitored with an optical pyrometer. The system was pumped with an ion pump. All measurements were conducted at pressures less than 10^{-8} torr.

C. *Measurement Technique*

To take the noise measurements, all the accelerating and control electrodes of the gun were tied together so that the system behaved as a pseudo diode. Figure 4 shows a typical current-temperature characteristic for fully space charge limited operation of a B-type cathode. The maximum current that could be drawn without overheating the anode structure was 5 mA corresponding to 1 A/cm^2 with 130 volts applied. Figure 5 is a schematic of the electronic instrumentation used. Caution was exercised in selecting the instrumentation so as to minimize the introduction of any further noise. All the instrumentation was powered through an isolation transformer to reduce line voltage fluctuations. The heater power was obtained from a highly stabilized dc supply (H.P. 6227B) to avoid effects due to fluctuating magnetic fields or changes in line voltage. The anode supply (Fluke 415B) was voltage stabilized to 1 part in 10^5. The diode current was measured with a digital ammeter (Keithly 177) to 5 significant figures. The current fluctuation noise was measured by passing the fluctuation through a 25 μF capacitor and across a 10 kΩ precision thin-film resistor. A high impedance JFET (Burr-Brown OPA-

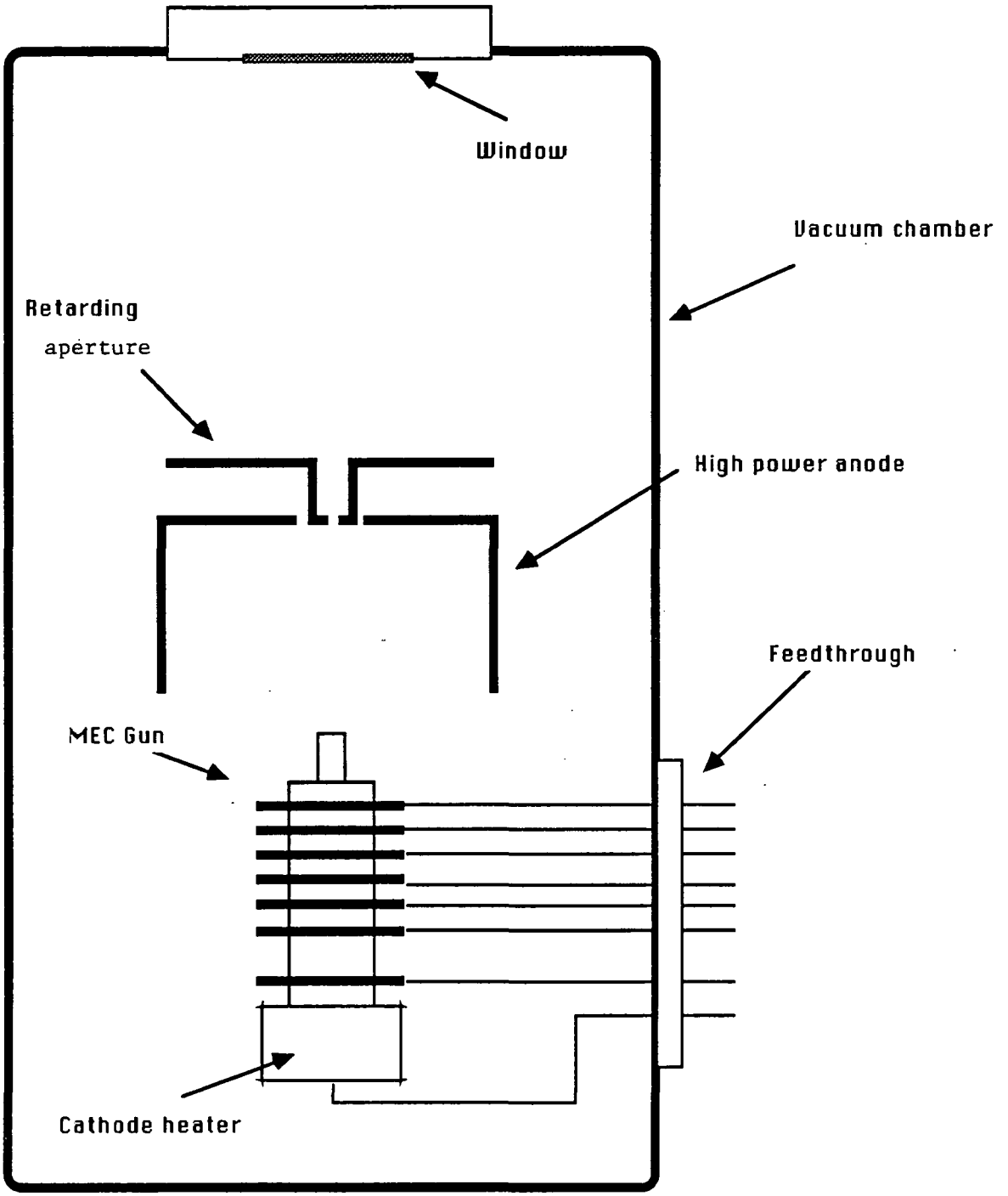

FIGURE 3 High-power gun testing system

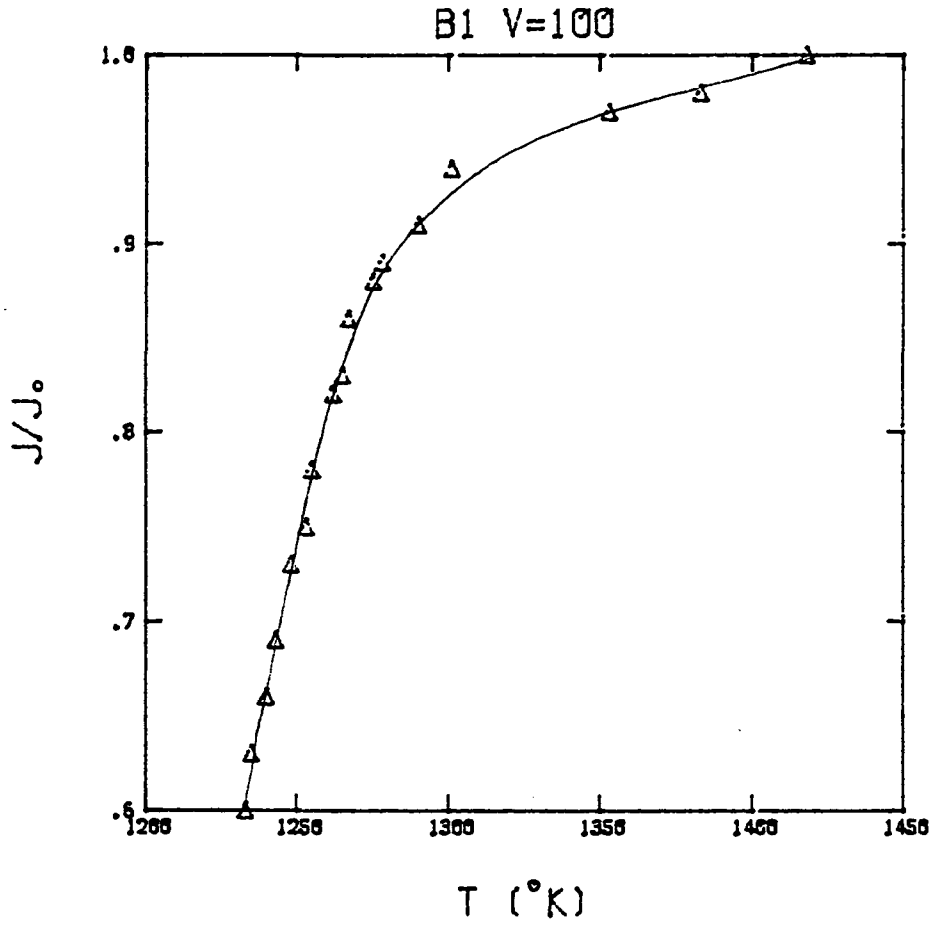

Figure 4 Typical current-temperature characteristics

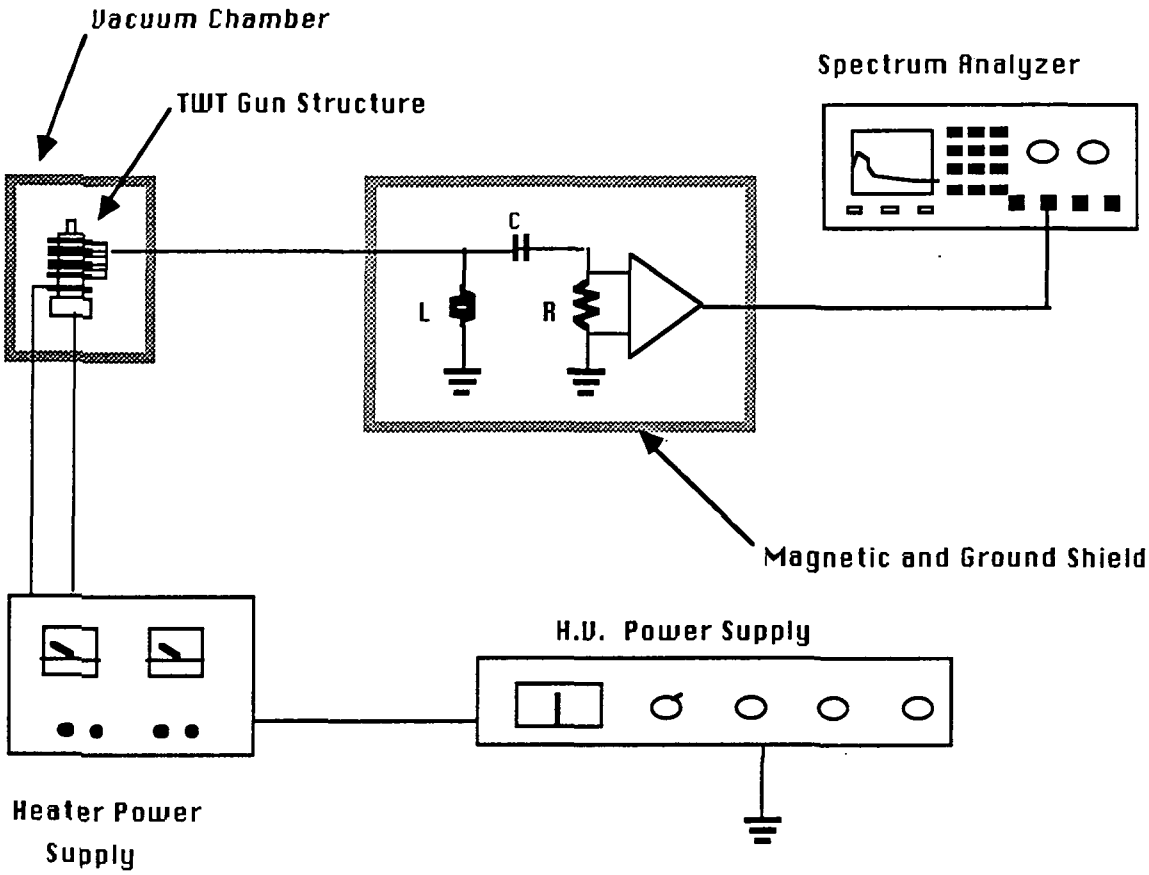

FIGURE 5 Electronic instrumentation

102) low noise wide band operational amplifier fed the signal into an H.P. 3582 spectrum analyzer. An average spectrum is obtained by multiple scanning of the frequency from 0 - 25 kHz, or 15 - 25 kHz for the shot noise region. The spectrum is stored by the instrument and can be displayed or plotted out. Figure 6 is a typical noise plot.

The square of the output from the spectrum analyzer is proportional to the rms current fluctuation, and since the bandwidth of the analyzer filter is known, it can be easily calibrated from the well-known shot noise equation. We used the rectangular bandpass filter so that

$$\langle i^2 \rangle_{SHOT} = eI\Delta f$$

where Δf is the bandwidth.

In estimating the cathode temperature from the optical pyrometer reading, we note that the window's transmission coefficient is constant in the region of interest. Since the cathode was too small to drill a black body hole in its surface, we used a spectral emissivity correction previously measured for B cathodes by Brodie.[4] We believe that the absolute error from this procedure does not exceed $\pm$ 5 K.

There are five measurable interrelated parameters, namely:

applied voltage	V (volts)
cathode emission density	J (amps cm^{-2})
cathode temperature	T (Kelvin)
current fluctuation noise	$\langle i^2(f) \rangle$ ($amps^2$)
frequency and bandwidth of noise measurement	f, Δf (Hz)

In general,

$$\langle i^2(f) \rangle = A.W\,(J, V, T, f)\,\Delta f$$

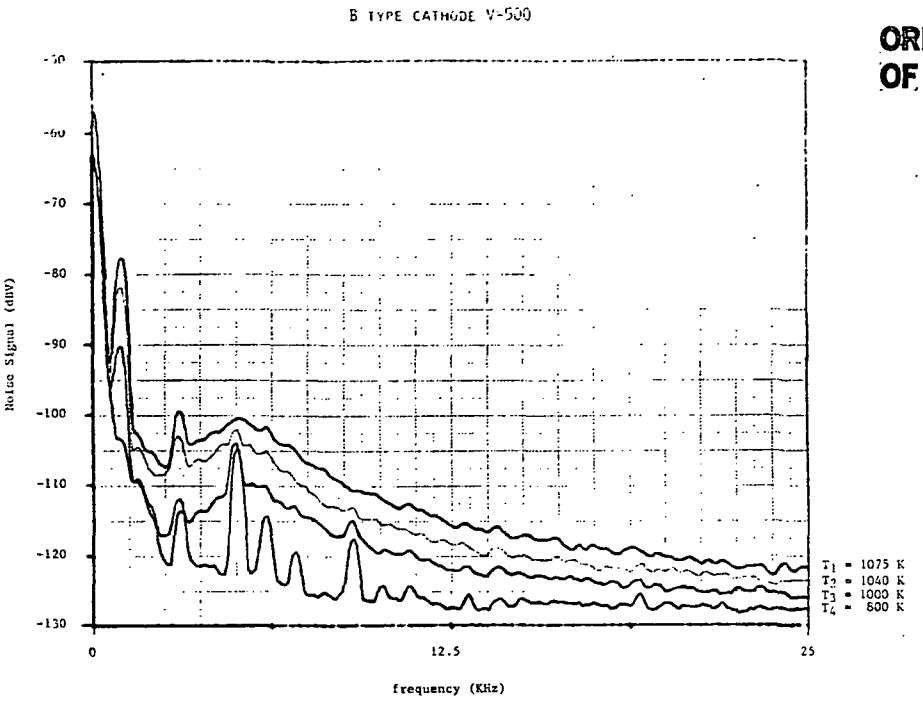

a) full noise spectrum

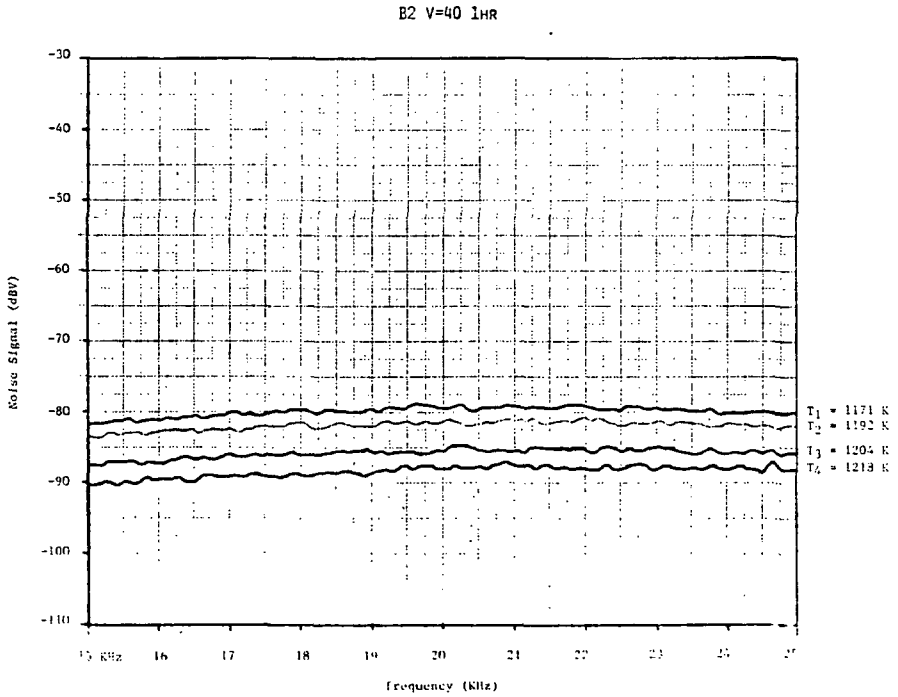

b) shot noise region

Figure 6 Typical noise plots from spectrum analyzer

where A is the cathode area and W is the noise intensity distribution function in units of $\left(\frac{\text{coul}^2}{\text{cm}^2\text{sec}}\right)$.

Our instrumentation yields $<i^2(f)>$ versus f (the noise spectrum) at fixed values of the other parameters. The experimental procedure depends on the particular type of information we are seeking. We note that V and J can be measured to a high precision, $<i^2(f)>$ can be measured to a fair degree of precision (2 - 3 significant figures) depending on the length of averaging time, and T can be measured within 10 K (3 significant figures).

Two cathodes of each type (B and M) were studied. They were designated B1, B2, M1, and M2. The principal noise measurement procedure was to fix the gun (diode) voltage at a specific value, usually 40 V, 100 V, or 130 V; the emission current was then held at a fixed value between zero and the fully space charge limited value (determined by the heater power). The temperature of the cathode was measured using an optical pyrometer. The noise spectrum was then measured over a frequency range from 15 kHz to 25 kHz using a 145 Hz bandwidth.

D. *Data Reduction Techniques*

The interrelation between the available variable parameters (V,J) and the fluctuating current noise $<i^2>$ allows two different perspectives of the noise characteristics, i.e., $<i^2>$ vs. V and $<i^2>$ vs. J. We chose to examine the noise distribution (W) as a function of current at certain fixed voltages as this enabled us to analyze the data more conveniently.

A typical plot of the noise intensity distribution function, W, is shown in terms of W′ versus J at 20 KHz in Figure 7; where W′ has not been corrected for the signal gain in the instrumentation (i.e., $W' \propto W$). It consists of three regions: (1) where the W versus J plot is linear indicating that all the current being drawn is temperature limited (TL), (2) where space charge is partially limiting the current and lowering the noise, and (3) where the diode is completely space charge limited (SCL) and only slightly affected by increasing the temperature. As a practical matter, we found that the range of region 3, between the lowest temperature for complete space charge limitation and the maximum temperature we could heat the cathode without burning out the heater (1200 K -

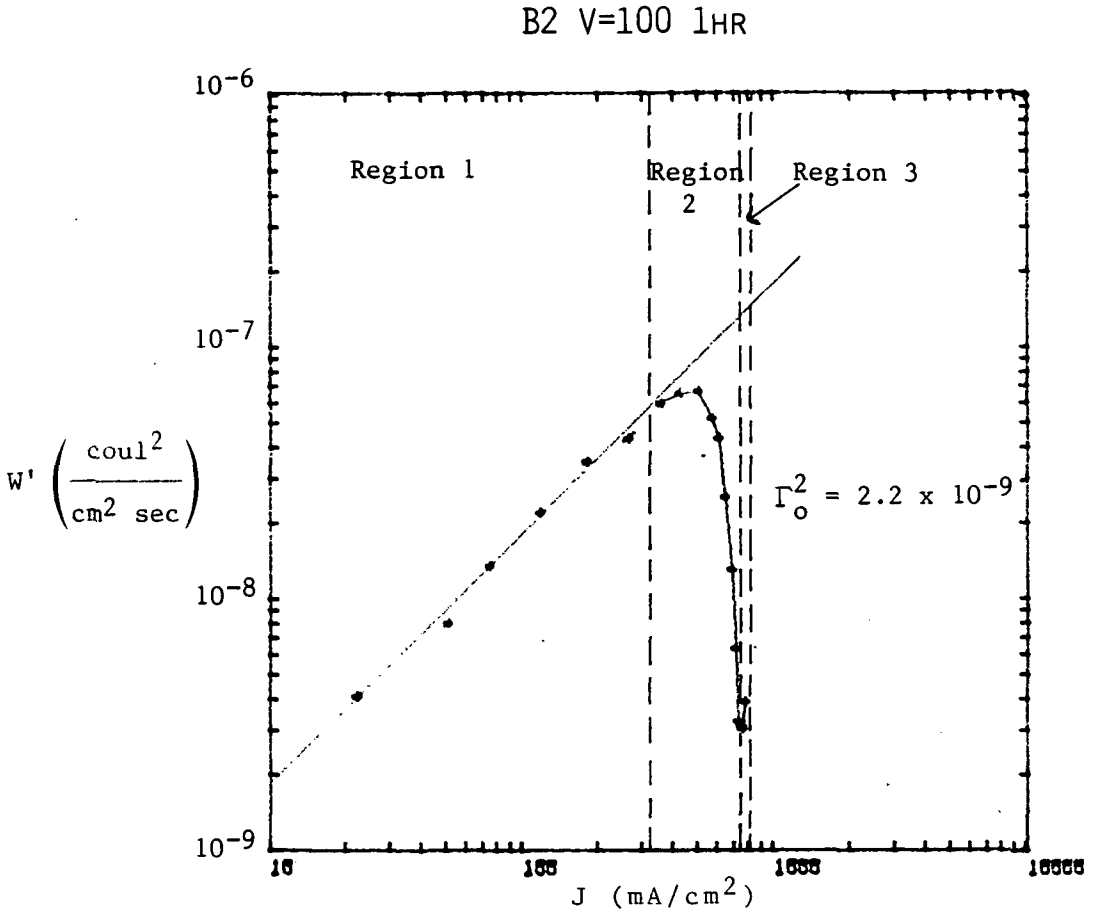

Figure 7 Typical noise intensity distribution, 20 KHz, Δf = 145 Hz

Region 1 corresponds to temperature limited,
Region 2 corresponds to partially space charge limited, and
Region 3 corresponds to completely space charge limited.

1400 K), was too small for meaningful measurements.

To analyze the partially space charge limited region, we assume that the cathode consists of patches of different work function, each behaving as its own simple diode. While this is obviously not exactly true as the patch becomes space charge limited, the Pierce correcting electrodes at the gun, the short cathode to anode distance, and the existence of current flow in adjacent patches all contribute to making this assumption substantially correct and consistent for measurements at the same voltage. We note that Tonnerre, et al.[5] use the same assumption in obtaining the work function distribution from the current voltage characteristics alone, in a situation where perhaps it is less justified since the effective d of a gun can vary with applied voltage due to movements of the equipotentials with partial space charge limitation. We further assume that the space charge limited current density and the noise space charge reduction factor (Γ^2) for each patch are the same as the final values achieved for the whole diode (J_0 and ${\Gamma_0}^2$). Hence if g = fraction of the surface that is space charge limited at a given current value, then the current density flowing through the diode can be expressed as

$$J = gJ_0 + (1 - g)J_{TL} \tag{1}$$

Similarly, the noise distribution function at a fixed current can be expressed in terms of the space charge reduction factor as

$$W = e\Gamma^2 J = e{\Gamma_0}^2 gJ_0 + e(1 - g)J_{TL} \tag{2}$$

Combining (1) and (2), we find that the fraction of the surface that is space charge limited is given by

$$g = \frac{J}{J_0}\,\frac{(1 - \Gamma^2)}{(1 - {\Gamma_0}^2)} \tag{3}$$

If J is changed to $J + \Delta J$ by increasing the cathode temperature by ΔT, then Γ^2 changes to $\Gamma^2 + \Delta(\Gamma^2)$ and

$$\Delta g = \frac{\Delta J(1 - \Gamma^2) - J\Delta(\Gamma)^2}{J_0(1 - \Gamma_0{}^2)} \tag{4}$$

where the term on the order of Δ^2 is negligible. Now Richardson's equation states that for a surface of work function ϕ

$$J(\phi) = 120.4T^2 \exp\left[-\frac{\phi}{kT}\right] \sim J_0 \tag{5}$$

which is the emission at zero field, for the region just passing from TL to SCL as the temperature is changed by ΔT.

Differentiating equation 5 with respect to T, we obtain

$$\Delta\phi = \frac{\phi}{T}\,\Delta T + 2k\Delta T \sim \frac{d}{T}\,\Delta T, \tag{6}$$

where the k term is several orders of magnitude smaller. We define $f(\phi)$ as the fraction of surface with work function between ϕ and $\phi + \Delta\phi$

$$\Delta g \equiv f(\phi)\Delta\phi \tag{7}$$

Then combining equations 4, 6, and 7, we obtain

$$f(\phi) = \frac{T}{\phi\Delta T}\left[\frac{\Delta J(1 - \Gamma^2) - J\Delta(\Gamma^2)}{J_0(1 - \Gamma_0{}^2)}\right] \tag{8}$$

From the W versus J plot, using equation 8 we can obtain a plot of $f(\phi)$ versus ϕ using the following procedure. For each point measure T, J, Γ^2, and compute ϕ from equation 5. Between points, obtain ΔJ and ΔT. At complete space charge limitation measure J_0 and $\Gamma_0{}^2$. We can then use equation 8 to compute $f(\phi)$ as a function of ϕ. During this first phase of the noise studies program, these computations were carried out by hand.

III RESULTS AND DISCUSSION

The work function distribution of B- and M-type cathodes has been investigated and expressed in terms of the work function. The overall accuracy of the measured work functions by this technique is $\pm$ .01 eV and is only limited by the precision with which the temperature can be measured. However, the resolution within a particular distribution profile is significantly higher. Cathode aging effects were examined in three ways: work function distribution ($f(\phi)$ vs. ϕ), current noise distribution ($<i^2>$ vs. J), and Miram curves[6] (J/J_0 vs. T). Our work function distributions are compared with those obtained by previous workers.

The measurements taken under normal electrostatic focusing conditions as in the operational TWT were found to be very erratic and unreproducible. This was attributed to induced vibrations in the vacuum column and gun by the turbo molecular pump used. Time did not allow remounting of this system on an ion pump. For this reason, all measurements discussed were taken in the pseudo diode configuration.

A. *B-Type Cathode*

Two B-type cathodes have been examined (designated B1 and B2). The two cathodes were tested early in life (B1 after 15 minutes of operation at T = 1440 K, and B2 after 1 hour operation at T = 1385K). The cathodes were then subjected to an accelerated life conditioning at T = 1400 K, V = 130 V, J approx 1 A/cm^2 (B1 for 600 hours, B2 for 130 hours) and then tested. The goal of these measurements was to observe the cathodes during their period of greatest surface activity (highest Ba evaporation rate) and measure the work function changes. Table 1 outlines the contribution of the major work function peaks for different applied voltages.

The agreement in observed work function peaks between different voltages for a given cathode age is very good. At this point, one must also note the significant differences in observed $f(\phi)$ for different voltages. We believe these differences illustrate that our measurement technique is more or less sensitive to different work functions and work function patch sizes depending on the applied voltage. This can be understood by

Table 1

MAJOR WORK FUNCTION CONTRIBUTIONS FOR B CATHODES

Gun	Age (hours)	Voltage	ϕ	$f(\phi)$	ϕ	$f(\phi)$	ϕ	$f(\phi)$	ϕ	$f(\phi)$
B1	0.25	40							2.12	28.0
		100			2.03	12.5			2.11	11.36
		130					2.07	26.0		
B2	1	40					2.08	9.48	2.12	10.52
		100					2.07	10.70	2.12	5.46
		130			2.03	4.20	2.07	14.81	2.13	7.10
	130	40	1.97	4.15	2.01	6.23	2.06	8.81		
		100	1.99	6.53			2.06	14.0		
		130	1.97	5.03	2.03					

recalling that the system is not a perfect plane parallel diode. Changes in voltage affect the position of the space charge minimum in front of the cathode, hence affecting the neighboring contributions and effective patch size of our ensemble of emitting diodes on the surface. Thus, it seems possible to tune the sensitivity to examine the specific work functions by changing the applied voltage. Figures 8 and 9 are work function distribution plots at specific voltages taken before and after aging.

The results for B1 are only available after initial activation. The data taken after long-term aging were taken incorrectly, and we did not have time to repeat them. The overall work function envelope is similar to that measured by Tonnerre et al.[5] and Jansen et al.[7] The effective work function average is 2.06 eV.

Remarkably, the noise technique shows much higher resolution in the work function distribution than the earlier techniques. Thus we are able to show different work function contributions not previously observed. However, these results, although high in work function distribution resolution, still represent a convolution of all the work function patches on the cathode. A deconvolution of these work functions might be possible through the voltage sensitivity tuning discussed earlier.

In addition to obtaining the work function distribution of the cathode, the noise technique can be useful for establishing optimum operating conditions. Figure 10 is a plot of the current noise distribution as a function of the total current density for B1 after the initial activation. The three expected regions are clearly observable (i.e. temperature limited, partial space charge limited, and fully space charge limited). In contrast with the corresponding Miram curves for the same data Figure 11, these measurements demonstrate the onset of space charge effects at a much lower cathode temperature. For example, for V = 100 volts, the onset of the temperature limited-space charge limited knee in the Miram plot corresponds to T = 1255 K and J = 580 mA/cm^2. On the other hand, the noise distribution illustrates the onset of space charge effects at T = 1200 K and J = 329 mA/cm^2. In addition, the Miram curve illustrates a premature temperature for fully space charge limited current (i.e. T = 1280 K and J = 680 mA/cm^2). The noise measurement does not demonstrate fully space charge limited operation until T = 1363 K and J = 707 mA/cm^2. The difference in the space charge noise reduction factors, Γ^2, for the two space charge limited currents is not as significant with $\Gamma^2 = .025$ and $\Gamma^2 = .015$ respectively for fully space charge limited operation. Thus, the noise measurement technique proves more sensitive than the Miram method

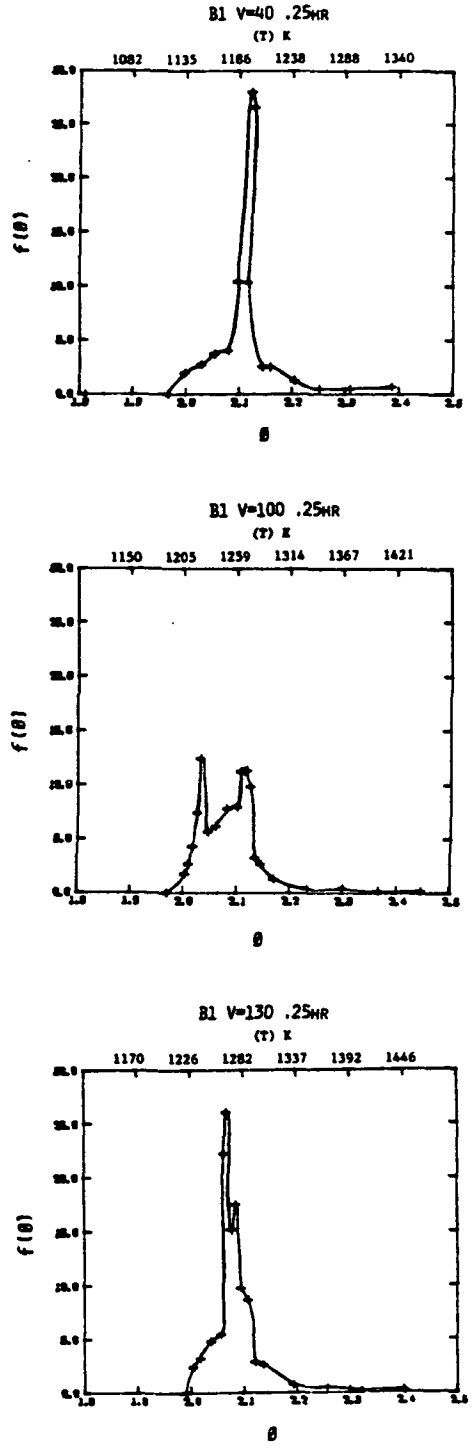

Figure 8 B1 cathode work function distribution before aging

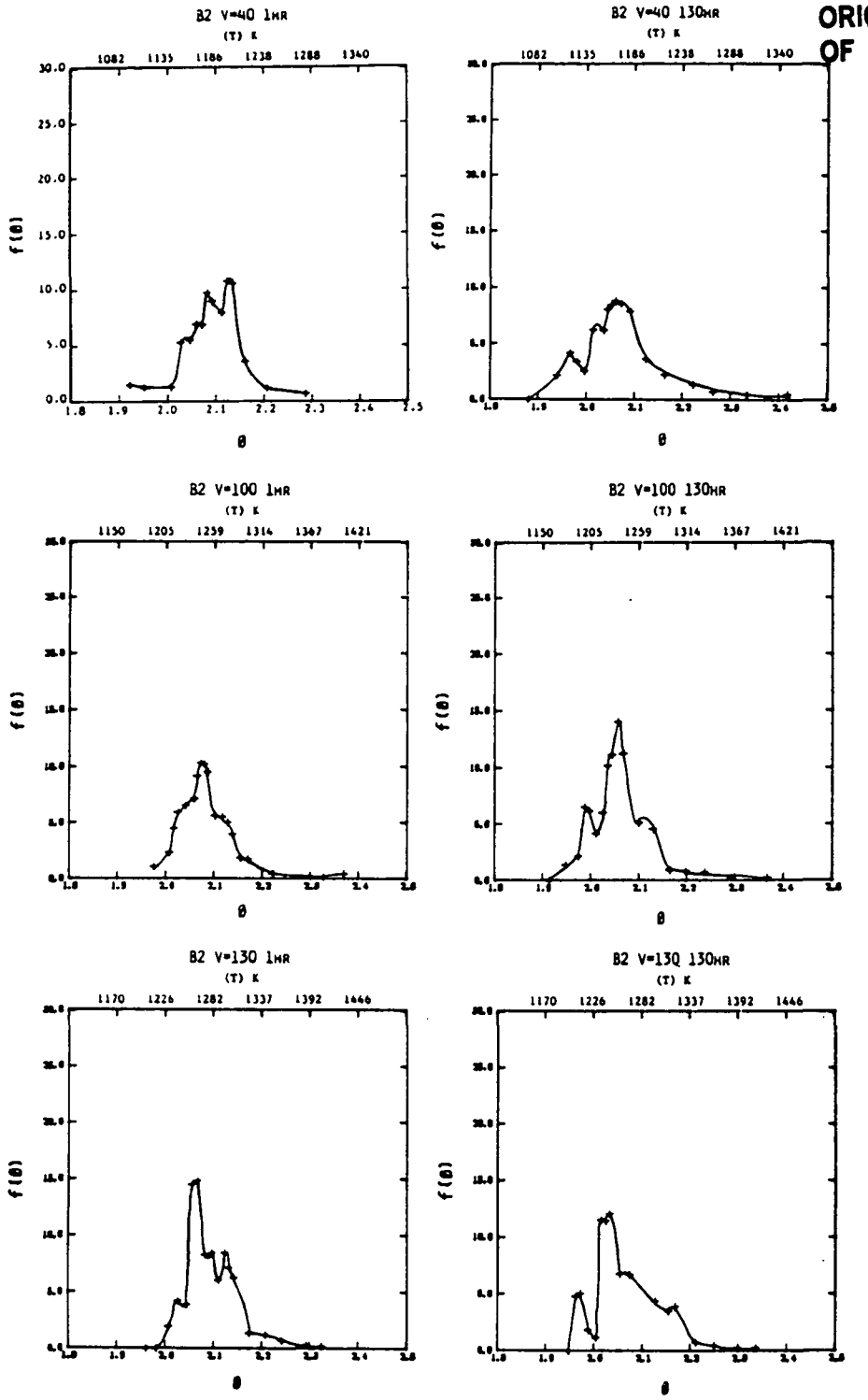

Figure 9 B2 cathode work function distributions before (1 hr.) and after aging (130 hrs.)

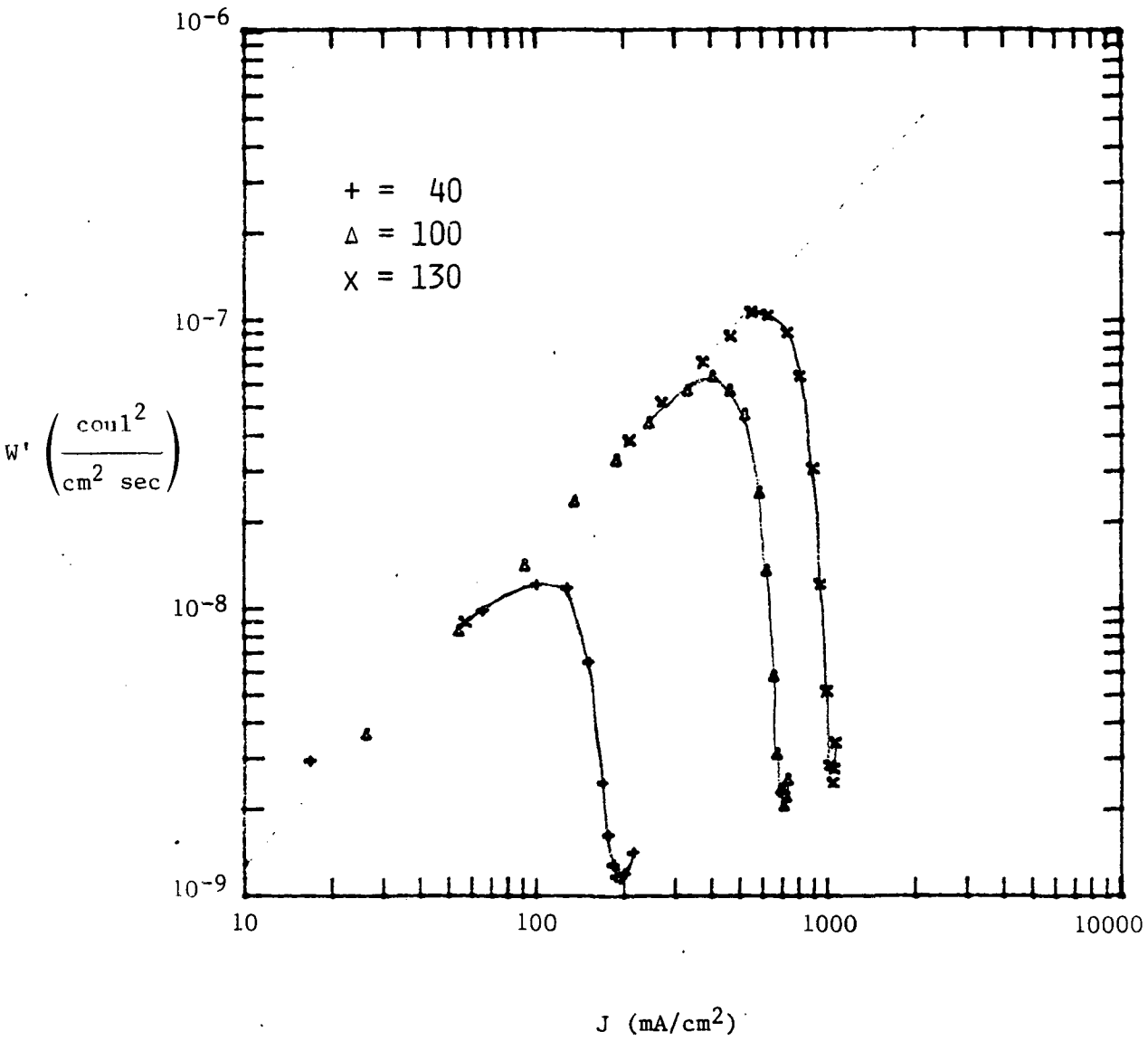

Figure 10 Current noise distribution for B1 after .25 hr.

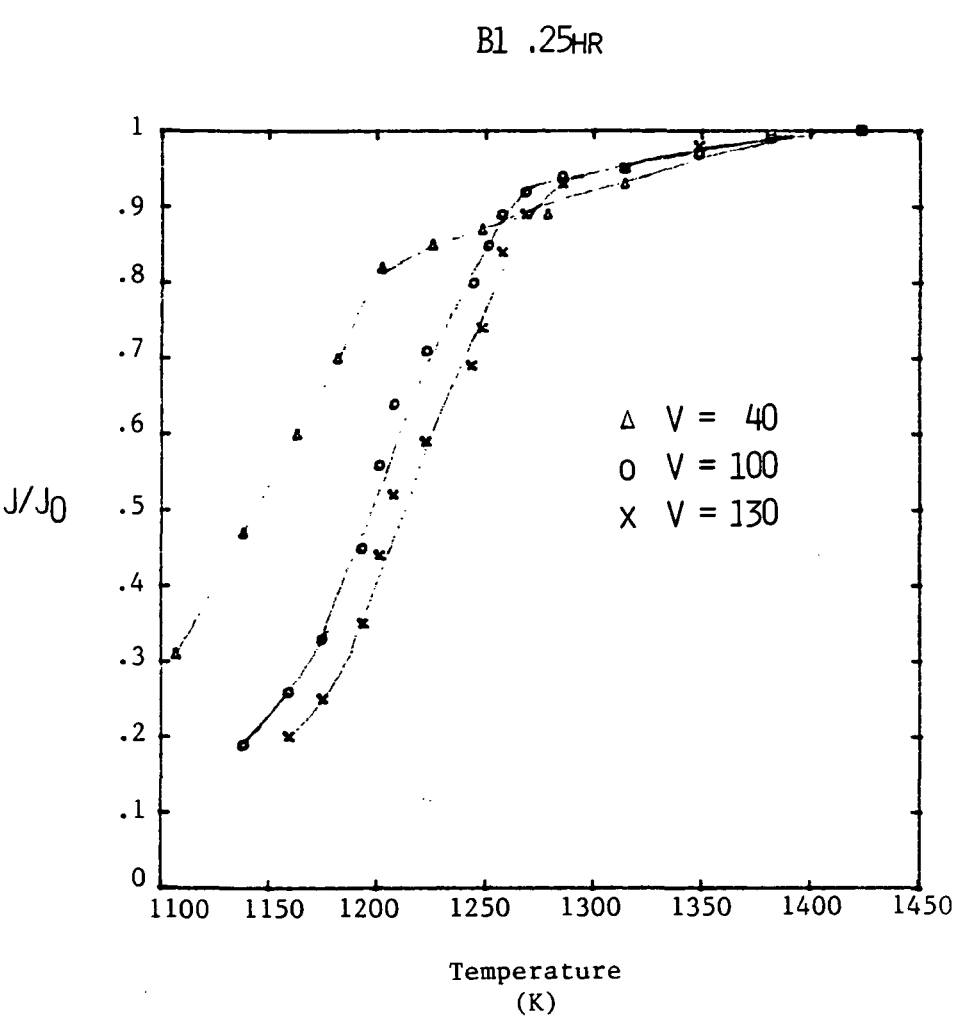

Figure 11 Miram type plot for B1

for detecting the onset of space charge effects.

The work function distribution for B2 (Figure 9) is significantly broader and shallower than that observed for B1 (Figure 8) but has the same effective work function average ($\phi \sim 2.06$ eV). However, the overall widths of work function envolopes are approximately equal.

Early in life, cathode B2, in contrast to B1, exhibits two very significantly different work function peaks at $\phi = 2.06$ eV and $\phi \sim 2.13$ eV. The Miram plots, however, do not illustrate the source of this difference. These work function contribution differences are most likely due to differences in the activity of the cathode surface.

Aging of the cathode at T = 1400 K for 130 hours changed the work function distribution. The contribution from the peak at $\phi \sim 2.13$ eV was significantly reduced. On the other hand, there was a significant increase in emission from a peak at $\phi = 1.97$ eV. This lower work function contribution did not exist at early life in either B1 or B2. The reason for these work function changes is probably due to an initial low activity of the pore endings containing the barium compounds ($\phi = 2.12$ eV) and subsequent activation of the same pore endings after aging leads to a lower work function ($\phi \sim 1.97$ eV). As can be seen by the remaining smaller contribution at $\phi \sim 2.12$ eV, activation of the pore endings is not complete. The intermediate contribution from work function of $\phi \sim 2.065$ eV corresponds to the remaining tungsten surface activated by Ba and BaO.

It is interesting to note that, visually, the current noise plots for the cathode do not appear to be very different before and after activation. There is a slight change in the curvature of the initial introduction to the space charge limited current region and a slight change in the slope of $<i^2>$ vs. J during the transition to fully space charge limited operation; however, when analyzed, the differences seem to be of major importance.

As with B1, the current noise distribution for B2 illustrates the onset of of space charge limited current occuring at a lower temperature and fully space charge limited current at a higher temperature than the corresponding Miram curves. However, the corresponding Miram curves do illustrate some changes after cathode aging.

B. *M-Type Cathodes*

Two M-type cathodes have been examined (designated M1 and M2). As with the B-type cathodes, these cathodes were tested early in life (M1 after 1 hour at T = 1420 K and M2 after 30 minutes at T = 1405 K). The cathodes were then subjected to an accelerated life conditioning of T = 1400 K (M1 for 150 hours and M2 for 190 hours at V = 130 V, J $\sim$ 1 mA/cm^2). Table 2 lists the contributions of the observed major work function peaks at different applied voltages.

The work function distributions for M1 and M2 are shown in Figures 12 and 13 respectively. It is important to note at this point that the temperature measured with the optical pyrometer could not be corrected for brightness as in the case of the B cathodes because the emissivity of this surface was not available. These uncorrected temperatures lead to displacements in the work function values (so as to indicate slightly lower values than the true values).

At early life, the agreement in work function contribution for each cathode at both voltages is very good. The overall envelopes of the work function are also very similar and have an average of $\phi \sim 2.075$ eV. This value is higher than would be expected for a M-type cathode. The reason for this, at present, is not well understood and might be due to a low activity of the cathode early in life.

After aging, there does exist a shift toward lower work function contributions. M1 clearly exhibits two distinct contributions at $\phi = 1.97$ eV and 2.04 eV. M2, on the other hand, although it exhibits a reduction in average work function to $\phi \sim 2.065$ eV, does not show the two work function states. It appears that after aging, M2 has its surface modified to a state similar to the initial state of M1. The reason for this is not clear and could be due to poisoning of the cathode surface. It is unfortunate that time did not allow for measurements at more extended cathode aging.

Table 2

MAJOR WORK FUNCTION CONTRIBUTIONS FOR M CATHODES

Gun	Age (hours)	Voltage	ϕ	$f(\phi)$	ϕ	$f(\phi)$	ϕ	$f(\phi)$	ϕ	$f(\phi)$
M1	1	100	2.00	6.62	2.03	13.20	2.06	12.60	2.08	11.74
		130	2.00	2.80	2.03	6.24	2.06	18.55	2.08	20.60
	150	100	1.97	6.15	2.04	14.40				
		130	1.96	10.00	2.02	14.20				
M2	.5	40	2.01	6.35			2.06	8.42	2.09	16.60
		100	2.01	5.37			2.08	8.80	2.10	15.88
	190	40					2.06	20.25		
		100					2.07	14.69	2.11	8.10

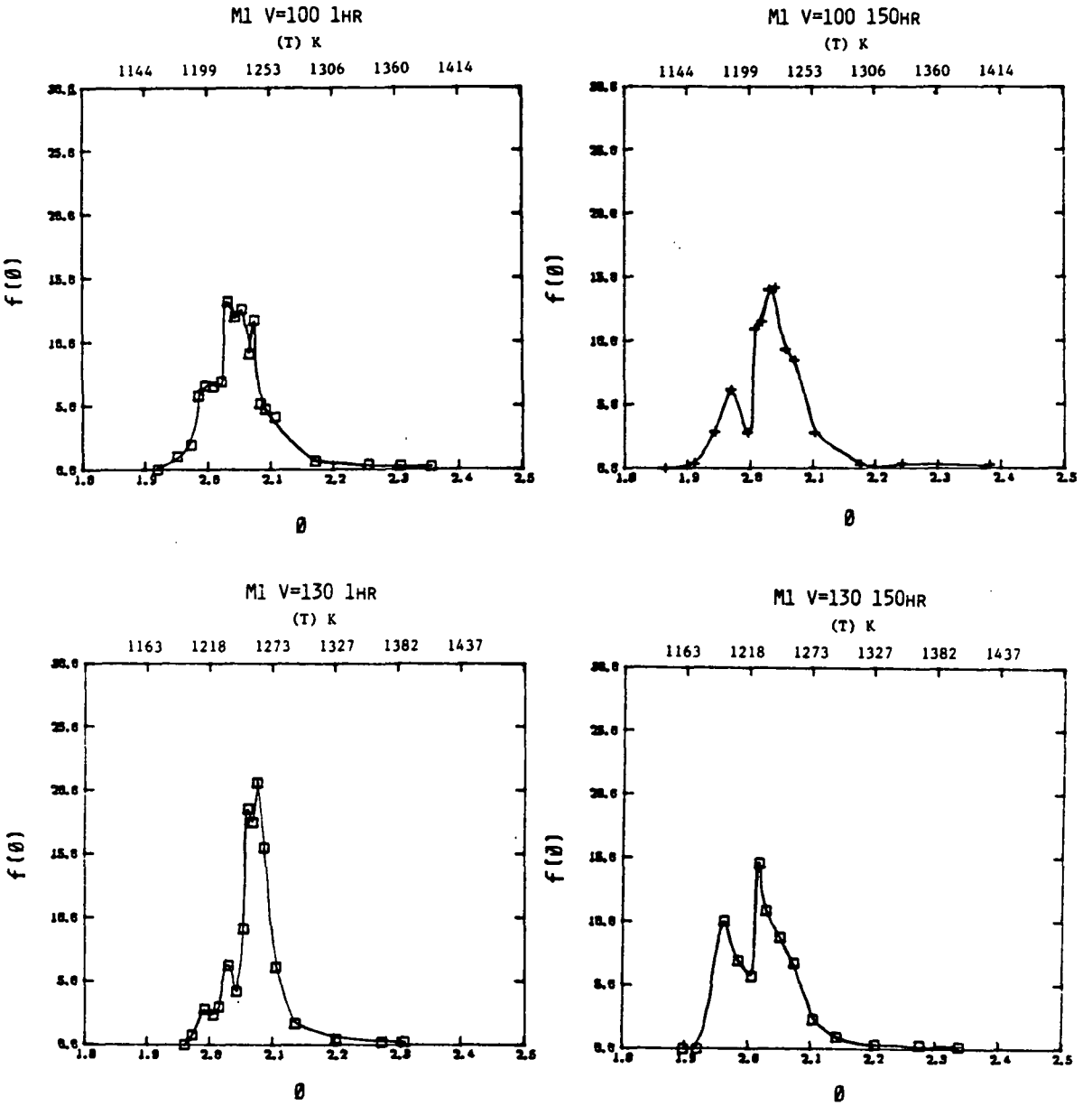

Figure 12 M1 cathode work function distribution

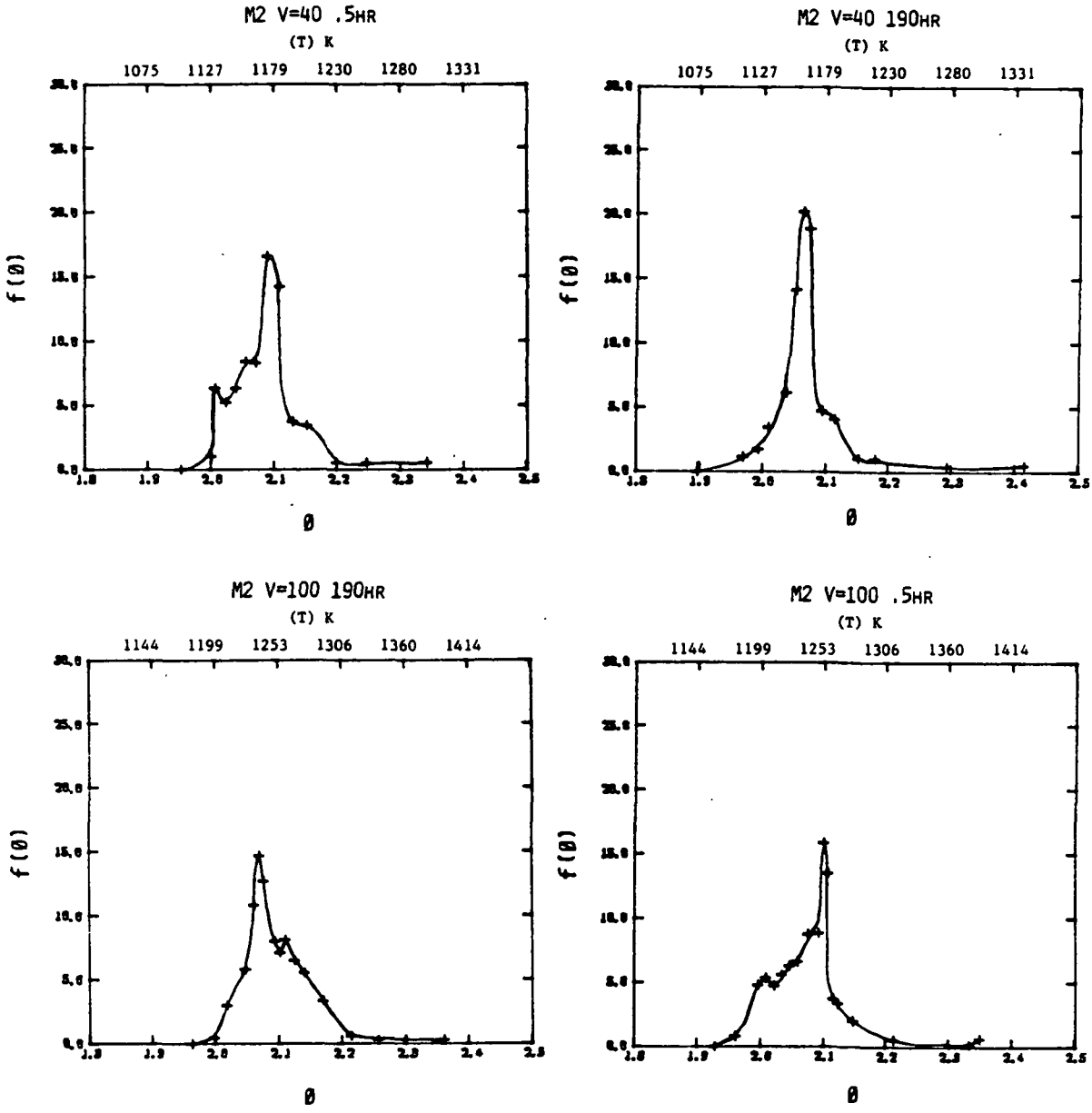

Figure 13 M2 cathode work function distribution

IV CONCLUSIONS

The technical objectives of this first phase of the project to explore the use of noise measurements to diagnose the condition of the cathode in an operating TWT were substantially accomplished. Two test stands were designed, built, and operated for handling TWT gun structures and which provided for the detection, recording, and analysis of the cathode noise signals, and for independently measuring the cathode temperature. Four barium dispenser cathodes (two type B and two type M) were analyzed by this technique.

The observed work function distribution of B-type cathodes were comparable to those observed by other workers and had an average $\phi = 2.06$ eV. The higher resolution obtained by this technique due to noise reduction of small patches illustrated many different contributions not previously observed. Aging effects were observed from the reduction in contribution at $\phi \sim 2.13$ eV and the emergence of a contribution at $\phi \sim 1.97$ eV. This is attributed to the activation of Ba pores in the W matrix. This technique also illustrated space charge effects over a broader temperature range than the Miram type curves.

The M-type cathodes also demonstrated a plurality of work functions not previously observed. These were centered about $\phi \sim 2.075$ eV. This value is higher than expected for M-type cathodes and might be due to poisoning. Aging did demonstrate a reduction is average work function. M1 unexpectedly exhibited both a high and low work function contributions after aging at, $\phi \sim 1.97$ eV and $\phi \sim 2.04$ eV.

This technique also demonstrated a voltage-dependent sensitivity to work function contribution. Lower anode voltages appear to be more sensitive to higher work function, and higher voltages more sensitive to the lower. Thus, it might be possible to use this voltage dependence to observe the presence of different contributions.

The computer automation of this technique would greatly enhance the resolution observed in the work function distribution. This would allow much more data to be taken to obtain a statistical base of work function distributions which could be used to compare with other cathodes and in cathode fabrication. In turn, these work function

distributions could be used to determine accurate cathode operating temperatures in TWT structures.

Noise measurements also demonstrated a higher sensitivity to space charge effects than the Miram method. Therefore, it is also possible to use this technique for establishing the optimum cathode operating conditions for TWT structures.

APPENDIX

The Theory of the Space Charge Limited Thermionic Diode

by: I. Brodie

3/13/85

A. *Introduction*

One of the more remarkable physical phenomena is the reduction in current fluctuation noise that occurs in a thermionic diode during the transition from the temperature-limited to the space charge-limited modes of operation.[8] Remarkable because random fluctuations, due to an initial Poisson distribution in the emission of discrete quanta of charge (electrons), are substantially reduced by subsequent correlation between the motion of electrons induced by space charge in their journey from cathode to anode.

In general, the mean square current fluctuation in a planar diode at frequency f in range Δf is given by

$$\langle i^2(f) \rangle = A.W\,(J, V_a, T, f)\,\Delta f \qquad (1)$$

where A is the a cathode area, W is the noise intensity distribution function, J is the current density passing through the diode when a potential difference of $+ V_a$ is applied, the cathode being held at temperature T K.

Figure 7 shows how W varies with the current density for a planar diode held at three different voltages. The cathode was a barium dispenser cathode[2] and the measurements[9] were made at f = 20 kHz Δf = 145 Hz. The current density was varied by varying the cathode temperature. It will be seen that at low currents where J is temperature limited, W is proportional to J; however, as the cathode temperature is increased beyond a certain point, the current density does not increase substantially above a value determined by the space charge limit at the applied voltage, and in this region W decreases by about two orders of magnitude. In the temperature limited range

at this frequency, the current fluctuations, termed the shot noise, are due to the discrete nature of the electron and the fact that they are randomly emitted from the surface of the cathode. The presence of the space charge minimum in front of the cathode in the space charge limited case produces some correlation between the arrival of electrons at the anode thereby reducing the current fluctuation noise. In the temperature limited mode, it may be shown[1] that with a rectangular bandpass filter, $W = eJ$, and in the space charge limited mode, the space charge reduction factor, termed Γ^2, is defined by $W \equiv \Gamma^2 eJ$.

A number of attempts have been made to predict theoretically the value of the space charge reduction factor.[8,10] The simplest theory, based on taking in account the velocity distribution of the electrons, predicts values of Γ^2 many orders of magnitude smaller than the values actually observed and has lead to sophisticated refinements[11] in attempts to resolve this discrepancy. The work reported here grew out of a need to program a computer to solve the space charge limited flow equations taking into account the velocity distribution of the emitted electrons corresponding to a cathode temperature T K. Although the equations are well known,[12] without the aid of a computer, they are extremely cumbersome to use. However, with the computer program we were able to verify, as shown in Section B below, that in practical situations the simple theory predicts $\Gamma^2 \sim 10^{-9}$ compared with measured values of $\Gamma^2 \sim 10^{-2}$. At the same time, the theory demonstrated that the current density was extremely sensitive to the diode spacing d. This led to the investigation of the effect of thermal length fluctuations on the diode spacing d reported here.

B. *Space Charge Limited Currents*

Consider a planar cathode at temperature T spaced distance d from a planar anode. With zero electric field at the cathode surface, the cathode is capable of emitting $J_0(T)$ A/cm^2. In the space charge limited region, a voltage $+ V_a$ applied to the anode only allows the diode to pass a current density of J amps/cm^2 ($J < J_0$) due to the existence of a potential minimum of value $-V_m$ that is formed in the plane distant x_m from the cathode.

If the electrons are emitted from the cathode with a Maxwell-Bolzmann distribution then

$$J = J_0 e^{-\frac{eV_m}{kT}} \tag{2}$$

where e is the electronic charge and k is Bolzmann's constant.

Defining

$$\eta \equiv \frac{e}{k}\left(\frac{V + V_m}{T}\right) \tag{3}$$

where V is the potential at a plane distant x from the cathode, and

$$\xi \equiv \left(\frac{(2m\pi)^{1/4}}{k^{3/4}}\,\frac{e^{1/2}}{\epsilon_0{}^{1/2}}\right) T^{-3/4} J^{1/2}(x - x_m) \tag{4}$$

where m is the electron mass and ϵ_0 is the permittivity of empty space;

Langmuir[12] has shown

$$\xi^{\pm} = \int_{u=0}^{\eta} \frac{du}{\left(e^u - 1 \pm e^u \mathrm{erf}(u^{1/2}) \quad 2(u/\pi)^{1/2}\right)^{1/2}} \tag{5}$$

where $\xi = \xi^+$ between the anode and potential minimum, i.e., for $x > x_m$, $\xi = \xi^-$ between the cathode and potential minimum, i.e. for $x < x_m$, and

$$\mathrm{erf}\left(u^{1/2}\right) = \frac{2}{\sqrt{\pi}} \int_0^{u^{1/2}} e^{-z^2}\, dz = \text{error function of } (u^{1/2}). \tag{6}$$

Thus at the cathode, from equation (3) and (4) and putting

$$A_0 = \left(\frac{(2m\pi)^{1/4}}{k^{3/4}}\,\frac{e^{1/2}}{\epsilon_0{}^{1/2}}\right) = 9.18642 \times 10^5 \text{ MKS units}$$

we have

$$\xi_c = A_0 T^{-3/4} J^{1/2} x_m = \int_0^{\eta_c} \frac{du}{\left(e^u - 1 - e^u \mathrm{erf}(u^{1/2}) + 2\left(\frac{u}{\pi}\right)^{1/2} \right)^{1/2}} \tag{7}$$

and from equation (2),

$$\eta_c = \frac{eV_m}{kT} = \ln J/J_0 \tag{8}$$

At the anode we have

$$\xi_a = A_0 T^{-3/4} J^{1/2} (d - x_m) = \int_0^{\eta_a} \frac{du}{\left(e^u - 1 + e^u \mathrm{erf}(u^{1/2}) - 2\left(\frac{u}{\pi}\right)^{1/2} \right)^{1/2}} \tag{9}$$

and

$$\eta_a = \frac{eV_a}{kT} + \frac{eV_m}{kT} = \frac{eV_a}{kT} - \ln J/J_0 \tag{10}$$

Solving for ξ_a in terms of the measurable variables V_a, T, J, J_0, and d, gives

$$A_0 T^{-3/4} J^{1/2} d + \int_0^{\ln[J_0/J]} f_1(u)du = \int_0^{\left[\frac{eV_a}{kT} + \ln J_0/J\right]} f_2(u)du \tag{11}$$

where

$$f_1(u) = \left[e^u - 1 + e^u \mathrm{erf}(u^{1/2}) - 2\left(\frac{u}{\pi}\right)^{1/2} \right]^{1/2} \tag{12}$$

$$f_2(u) = \left[e^u - 1 - e^u \mathrm{erf}(u^{1/2}) + 2\left(\frac{u}{\pi}\right)^{1/2} \right]^{1/2}$$

To shorten the integration time, we used the formula[13]

$$\mathrm{erf}\, x = 1 - \left(a_1 t + a_2 t^2 + a_3 t^3 + a_4 t^4 + a_5 t^5\right) e^{-x^2} + \epsilon(x),$$

where $t = \frac{1}{1 + px}$, $|\epsilon(x)| < 1.5 \times 10^{-7}$, $p = .32759\ 11$, $a_1 = .25482\ 9592$, $a_2 = -.28449\ 6736$, $a_3 = 1.42141\ 3741$, $a_4 = -1.45315\ 2027$, and $a_5 = 1.06140\ 5429$.

Given four of the five measurable variables (J, J_0, T, d and V_a) the computer was programmed to adjust the fifth until both sides of equation (11) differed by less than 1 part in 10^5.

By making a small change in J_0, the corresponding change in J (with T, d, and V_a held constant) could be computed, thus obtaining $\left(\frac{\partial J}{\partial J_0}\right)$.

Now

$$\Delta J = \left(\frac{\partial J}{\partial J_0}\right) \Delta J_0$$

Hence

$$\Delta J^2 = \left(\frac{\partial J}{\partial J_0}\right)^2 \Delta J_0^2$$

The mean square fluctuation on J_0 in frequency range f to f + Δf due to shot noise is given by

$$\langle \Delta J_0^2 \rangle_{av} = 2eJ_0\Delta f, \text{ and on J by, } \langle \Delta J^2 \rangle_{av} = \Gamma^2 2eJ\Delta f \text{ (by definition of } \Gamma^2)$$

Hence

$$\Gamma^2 2eJ\Delta f = \left(\frac{\partial J}{\partial J_0}\right)^2 2eJ_0\Delta f$$

or

$$\Gamma^2 = \left(\frac{\partial J}{\partial J_0}\right)^2 \frac{J_0}{J} \tag{13}$$

For the diode of Figure 7, using
$V_a = 100$ V, $J_0 = 10^5$ A/m^2, $J = 7700$ A/m^2, $T = 1300$ K, we compute
$d = 5.7 \times 10^{-4}$m and $\frac{\partial J}{\partial J_0} = 1.7 \times 10^{-5}$ leading to $\Gamma^2 = 3.75 \times 10^{-9}$.

The problem with the theoretical approach in arriving at equation (13) is that it does not take into account the time it takes for a change in J_0 to be reflected in a change in J. This is because the basic theory gives the value of J only after dynamic equilibrium has been reached. If the time constant to reach equilibrium is τ_0, then the above theory will be valid only for frequencies $f << \frac{1}{\tau_0}$. A rough measure of τ_0 may be obtained by estimating the transit time from the cathode to the potential minimum for an average electron that contributes to the total current J. Then $\tau_0 \sim \frac{x_m}{v_a}$ where v_a is the average velocity of electrons that can cross the potential minimum. Now

$$v_a > \left(\frac{eV_m}{m}\right)^{1/2}$$

hence

$$\tau_0 < x_m \left(\frac{m}{eV_m}\right)^{1/2} \tag{14}$$

V_m can be obtained from equation (7) and x_m from equation (6) using the computer program. For the example cited above, we obtained

$$-V_m = 0.31 \text{ volts, } x_m = 6.1 \times 10^{-6}\text{m, giving } \tau_0 \sim< 2.6\text{x}10^{-11} \text{ seconds}$$

Thus we would expect equation (13) to be valid for frequencies up to about 10 GHz, unless a detailed consideration of electron trajectories shows the rough estimate of τ_0 given above to be seriously in error. Since the experimental measure of Γ^2 (Figure 7) was made at only 20 kHz, it seems unlikely that transit time effects could be involved in this example. *It thus appears likely that there is some other noise generating mechanism that dominates before full space charge suppression of the shot noise is attained.*

In this regard it was noted that the sensitivity of J to changes in d can be very high. In general, the mean square fluctuation in J due to this effect is given by

$$<\Delta J^2>_{av} = \left(\frac{\partial J}{\partial d}\right)^2 <\Delta d^2>_{av} \tag{15}$$

For any set of variables $\left(\frac{\partial J}{\partial d}\right)$ can be obtained from the computer program. However to obtain an approximate value we note that for $x_m << d$, J is proportional to $\frac{1}{d^2}$

hence

$$\left(\frac{\partial J}{\partial d}\right) = \frac{2J}{d} \tag{16}$$

Comparing values obtained on the computer program with that of equation (16) has shown that this simplification is justified for most practical cases. Thus, if d is fluctuating with a mean square displacement $<\Delta d^2>_{av}$

then

$$<\Delta J^2>_{av} = \frac{4J^2}{d^2} <\Delta d^2>_{av} = \Gamma^2 2eJ\Delta f \text{ by definition of } \Gamma^2 \qquad (17)$$

Hence

$$<\Delta d^2>_{av} = \frac{d^2\Gamma^2 2e\Delta f}{4J} \qquad (18)$$

For the B cathode used to obtain Figure 7, we were able to estimate $d = 5.7 \times 10^{-4}$m from the space charge limited current ($J = 7700$ A/m^2) with an applied potential of 100 volts, the cathode held at 1300 K, and assuming $J_0 = 10^5$ A/m^2 (10 A/cm^2). Using this value of d, $\Delta f = 145$ Hz, $\Gamma^2 = 2.2 \times 10^{-2}$, and $J = 7700$ A/m^2. We obtain from equation (18)

$$(<\Delta d^2>_{av})_{RMS} = 3.2 \times 10^{-5} \text{ Å}$$

It seems reasonable that such a small displacement might be due to thermal fluctuations in length of the cathode modulating the diode spacing d. This possibility is discussed in Section C below.

C. *Thermal Elastic Fluctuations in the Length of a Rod*

The mean square amplitude of an elastic wave of frequency f, in a body at temperature T K consisting of N atoms of mass m, arranged in a lattice is given by[14]

$$<a^2(f)>_{av} = \frac{2}{mN} \cdot \frac{kT}{4\pi^2 f^2} = \frac{2kT}{\rho V 4\pi^2 f^2} \qquad (19)$$

where ρ = density and V = volume.

The incremental number of such energy bearing waves modes of longitudinal vibrations in the frequency range f to f + Δf is given by[15]

$$\Delta N = \left(\frac{4\pi V f^2}{c^3} + \frac{\pi S f}{2c^2} + \frac{L}{2c} \right) \Delta f \tag{20}$$

where S = surface area, L = sum of the three dimensions of the region under consideration, c = velocity of sound in the medium = $\sqrt{\frac{E}{\rho}}$, E = Young's modulus.

For a rod the mean square displacement of the end planes over the frequency range f to f + Δf is

$$<\Delta d^2>_{av} = \sum_{f}^{f+\Delta f} <a^2(f)> = \Delta N <a^2(f)> \quad \text{for } \Delta f << f \tag{21}$$

Hence using (19) and (20),

$$<\Delta d^2>_{av} = \frac{kT\Delta f}{4\rho\pi c} \left(\frac{8}{c^2} + \frac{S}{c^2 V f} + \frac{L}{\pi f^2 V} \right) \tag{22}$$

The cathode and support structure used for obtaining the data of Figure 7 were of rather complex shape; however, for the purposes of calculation, it may be approximated to a cylinder of length l = 1.37 x 10^{-3}m and radius r = 3.81 x 10^{-4}m giving

$$L = 2.13 \times 10^{-3}\text{m}, \; S = 4.19 \times 10^{-6}\text{m}^2, \; V = 6.25 \times 10^{-10}\text{m}^3.$$

Additional values for the cathode of Figure 7 (MKS units) are T $\simeq$ 1300 K (in space charge limited range), c $\simeq$ 5.4 x 10^3 m/sec (drawn tungsten),[10] f = 2.0 x 10^4 Hz, k = 1.4 x 10^{-23} joule/K, Δf = 145 Hz, $\rho \simeq$ 1.5 x 10^4kg/m^3 (80% that of tungsten to simulate the material of the dispenser cathode), J_{SCL} = 7700 A/m^2 with V_a = 100 volts, d = 5.7 x 10^{-4}m (computed).

Putting the appropriate values into equation (23), we obtain

$$(<\Delta d^2>_{av})_{RMS} = 3.08 \times 10^{-5}\text{Å}$$

in remarkable agreement with the value of 3.2×10^{-5}Å obtained by assuming that the measured current fluctuation in the space charge limited mode were due to fluctuations in the diode spacing (equation 18).

If we combine equations (18) and (22), we obtain

$$\Gamma^2 = \frac{JkT}{2d^2e\rho\pi c}\left(\frac{8}{c^2} + \frac{S}{cvf} + \frac{L}{\pi f^2}\right) \tag{23}$$

The variation of Γ^2 with the other parameters predicted by equation (23) may be experimentally verified. We note that equation (23) predicts:

1. That Γ^2 is independent of Δf.
2. At high frequencies,

$$\Gamma_h^2 \rightarrow \frac{4JkT}{d^2e\rho\pi c^3} \tag{24}$$

i.e. Γ_h^2 is independent of frequency and cathode shape.

3. At low frequencies,

$$\Gamma_l^2 \rightarrow \frac{JkTL}{2d^2e\rho\pi^2f^2Vc} \tag{25}$$

i.e., Γ_l^2 has a $1/f^2$ variation at fixed J and T.

4. The changeover from high to low frequency range occurs when

$$\frac{8}{c^2} = \frac{L}{\pi f_c^2 V} \quad \text{i.e.} \quad f_c = \left(\frac{Lc^2}{8\pi V} \right)^{1/2} \tag{26}$$

5. For a given diode at any fixed frequency, Γ^2 is proportional to JT.

The data of Figure 10 verifies Γ^2 is proportional to J at constant T. Additional data is required to verify the other predictions.

REFERENCES

1. Kaisel, S.F., R.E. Thomas and A.S. Gilmour, 1978: Test and Evaluation Committee Report, 1st Tri-Service Cathode Workshop, Naval Research Laboratory, Washington, D.C.

2. Levi, R., 1955: "Improved Dispenser Cathode," *J. Appl. Phys. 26*, p. 639.

   Brodie, I. and R.O. Jenkins, 1956: "Impregnated Barium Dispenser Cathodes Containing Strontium or Calcium Oxide," *J. Appl. Phys. 27*, p. 417.

3. Zalm, P. and A.J.A. van Stratum, 1966: "Osmium Dispenser Cathodes," *Philips Tech. Rev., 27*, p. 69.

4. Brodie, I., 1959: "Physical Processes in Ba Dispenser Cathodes," London University PhD Thesis.

5. Tonnerre, J.C., D. Brion, P. Palluel and A.M. Shroff, 1983: "Evaluation of the Work Function Distribution of Impregnated Cathodes," *Applications of Surface Science, 16*, pp. 238-249.

6. Grant, T.J., 1984: "A Powerful Quality Assurance Technique for Dispenser Cathodes and Electron Guns," *IEDM.*

7. Jansen, C.G.J., A. Venema, and Th. H. Weekers, 1966: "Nonuniform Emission of Thermionic Cathodes," *J. Appl. Phys., 37*, No.6.

8. Quate, C.F., 1959: "Shot Noise From Thermionic Cathodes," Chapter 1 of *Noise in Electron Devices*, (eds. L.D. Smullin and H.A. Haus) John Wiley.

9. Brodie, I., 1961: "Emission Fluctuations of Tungsten Based Barium Dispenser Cathodes," *J. Appl. Phys. 32*, pp. 2039-2046.

10. Bell, D.A., 1960: "Electrical Noise," *Van Nostrand*, pp. 129-147.

11. Petridis, V. and P.A. Lindsay, 1975: "New Formulation of Noise in Collision Free Systems," *Int. J. Electron. 38*, pp. 293-329.

12. Langmuir, I., 1923: "The Effect of Space Charge and Initial Velocities on the Potential Distribution and Thermionic Current Between Plane Parallel Electrodes," *Phys. Rev. 21*, pp. 419-435.

13. Abramowitz, M. and I.A. Stegun, 1964: *Handbook of Mathematical Functions*, Dover, p. 299.

14. James, R.W., 1948: *The Optical Principles of the Diffraction of X-Rays*, G. Bell, London, pp. 199-201.

15. *American Institute of Physics Handbook-(Third Edition, 1972)*, McGraw Hill, pp. 3-104.